Project Report

SCEC Project #21095

Experimental Investigation of Multi-Scale Flash Weakening – Continuation Project

Frederick M. Chester
Judith S. Chester
Monica Barbery
Santa Bonnett

Department of Geology & Geophysics
Center for Tectonophysics
Texas A&M University

Research Category: **Integration and Theory**

Science Objectives: **P1d, P3c, P2d**

Duration: **1 February, 2021 to 31 January, 2023**

Introduction

It is well established that for quasi-static friction, rate-dependence and fading memory behavior arises from time-dependent strength of micrometer scale asperity contact populations on sliding surfaces (e.g., Dieterich, 1978; Rice and Ruina, 1983). Direct observation and study of asperity contacts loaded statically and during sliding is difficult. Optical investigation of contact populations by static loading of transparent materials (Dieterich & Kilgore 1994; 1996) show that contact development involving both elastic and time-dependent yielding (indentation creep) produce irregular shape contacts, clusters of contacts that infill and coalesce, and a linear relation between true contact area and macroscopic normal stress. For quasi-static sliding in rock at high normal stress, true area of contact can be quantified by use of thermal dyes applied to a small fraction (3 %) of the sliding surfaces in triaxial shear friction experiments (Logan & Teufel, 1986). The experiments were conducted on precut, ground surfaces in a fine-grain quartz-rich rock (Tennessee sandstone), limestone (Indiana limestone), and in bi-material configuration, to document asperity contact dimensions during sliding. For the sandstone, asperity contact dimensions range up to .04 mm^2 (equivalent diameter of 0.22 mm) comprising a true contact area up to 10% area at a macroscopic normal stress of 200 MPa. For all rock-type combinations, area of individual asperity contacts is not directly related to the grain size of the rock. Calculated normal stress at sliding asperity contacts in the sandstone are on the order of 2 GPa over the range of macroscopic normal loads tested. Logan and Teufel (1986) also show that true area of contact increases linearly with macroscopic normal stress in all experiments, consistent with the linear relations documented for static loading conditions (Dieterich & Kilgore, 1994).

Continuing our research on flash-weakening friction in granite, this project report addresses our investigations of the true area of contact at asperities during high-speed slip. During our high-acceleration and high-speed sliding experiments on granite, load-bearing contacts undergo flash heating at the true contact interfaces, but with relatively little heating of the substrate, leading to a dramatic reduction in friction by flash weakening (Beeler et al., 2008; Rice, 2006). Using an apparatus with a pneumatic loading system coupled with a hydraulic damper, we are able to achieve relatively constant sliding velocities within the range of < 0.1 to 1 m/s with a maximum displacement of 35 mm. Moreover, our apparatus is capable of high acceleration to the target velocity, achieving a step velocity from quasi static to 1 m/s within ~3 ms. We employ a double-direct shear configuration with sliding surface area of 50x75 mm on each side of the central block, and use a high-speed IR thermal camera to capture images with a resolution of 50 µm/pixel at 3 ms intervals as the central block slides and emerges from the side blocks. The sequential images from a single-experiment records the flash-temperature over an area of 17 mm in width and 35 mm in length. We generally conduct repeat experiments using four different temperature ranges to document flash temperatures completely.

Work prior to this contract period has involved high-speed sliding experiments using granite blocks that are machined either flat or machined with a series of ridges and grooves. Thermal imaging documents that flash heating is inhomogeneous, and characterized by high-temperature mm-scale spots and streaks on the rock surface (Fig. 1). The thermal streaks and

spots in our high-speed experiments on granite are approximately an order of magnitude wider than streaks observed in quasi-static sliding experiments on Tennessee sandstone by Logan & Teufel (1986), and two orders of magnitude wider than contact spots seen in statically loaded transparent materials by Dieterich & Kilgore (1994, 1996).

Our grooved samples facilitate thermal modeling by knowing the macroscopic contact history produced by the grooves and ridges, records of macroscopic normal stress and velocity, and by using observed surface temperature and 1-D heat conduction modeling (Archard, 1959) combined with the flash-weakening relation (Rice, 2006) to determine the local normal stress distributions on the thermally imaged portion of the sliding surfaces (see Barbery et al., 2021).

Accomplished Tasks

1) We have conducted sliding experiments at normal stress between 2 to 20 MPa with IR thermal imaging to document surface temperature distributions during sliding, which are indicative of high-load bearing contacts, to determine the true area of load-bearing contact as a function of the macroscopic normal stress. Examples of thermally imaged load bearing contacts for macroscopic normal stress conditions of 3 to 15 MPa are shown in Fig. 1. Because the

Figure 1. Representative *IR* thermographs showing the measured surface temperature on the moving-block surface. Tests involved sliding under a macroscopic average normal stress indicated above figures. Images are near the end of sliding for measurement of contact areas at temperatures above 70˚C (a-d) and 80˚C (e), represented by colors of orange to white and tan, identify local normal stress greater than 40 MPa.

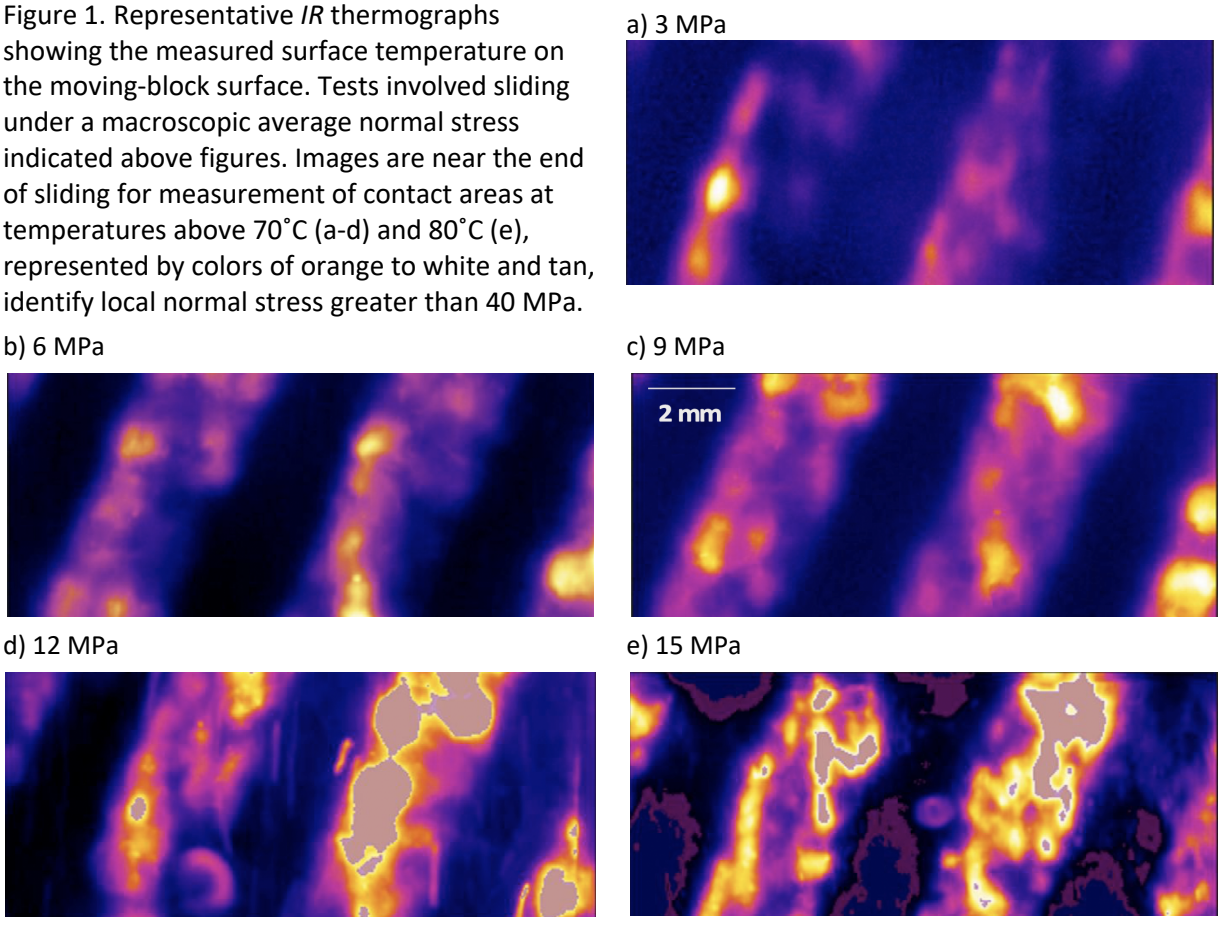

imaged area is small relative to the total are of the sliding surface (about 10 %), and that we find repetitive patterns of hot spots in successive experiments, we image four different areas of each block with at least two different temperature ranges so that we can sample a greater total area for each normal stress condition. As well, we are conducting experiments to higher normal stress by reducing the grooved area and beveling corners of the blocks to minimize stress concentrations and mitigate spalling and premature failure of the blocks.

Our measurements of true contact area are based on isotherm mapping relative to macroscopic normal stress magnitude (Fig. 1) as well as through coupled thermal- and flash-weakening friction modeling to robustly determine local normal stress magnitudes. Herein, we show the results of isotherm mapping of contacts for both flat ground surfaces (Fig. 2b) and grooved surfaces (Fig. 2c) compared to optical imaging of static contacts in transparent materials (Fig. 2a). In all cases, static and dynamic, true contact area increases linearly with macroscopic normal stress.

Figure 2. Comparison of a) true contact area for static µm-scale contacts (Dieterich & Kilgore, 1994), b) true contact area for sliding mm-scale contacts on flat-ground granite surfaces at m/s slip rate (Saber, 2017), c) true contact area for sliding mm-scale contacts on grooved-ground granite surfaces at m/s slip rates. In all cases true contact area increases linearly with normal stress

a)

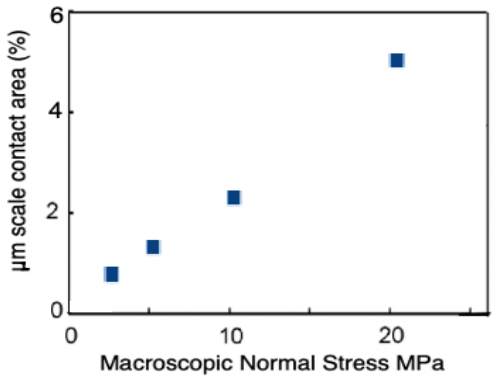

b)

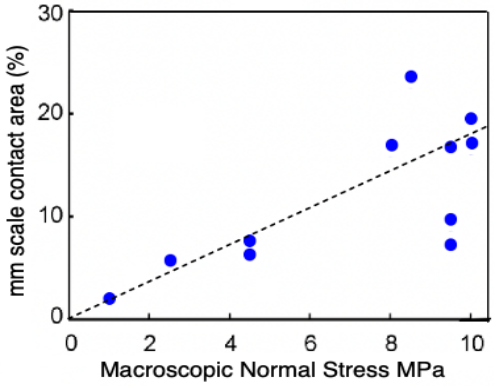

c)

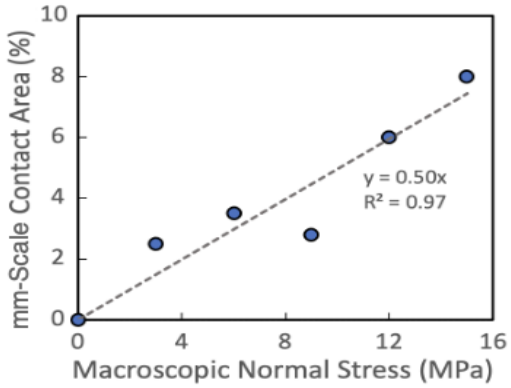

2) An important observation of hot spot distribution captured by IR thermal imaging is the similarity in hot spot patterns in successive experiments on the same granite blocks. Our procedure is to conduct about 6-8 experiments on a sample block before regrinding the groove and ridge pattern and finishing the flat ridge surfaces. After each test we gently brush the small chips and fine-grained wear product off the block surfaces using a soft-bristle, camel-hair artist

brush. The majority of the fine wear product adheres to the sliding surfaces and forms striations with widths on the order of 1-2 mm, similar to the dimensions of hot spots in thermal images. In addition, we have used thermal modeling analysis to determine local normal stress patterns, and find that initial sliding tests on newly prepared sample blocks show narrower hot spot tracks and temperature distribution indicating very high local normal stress at early sliding, and broader, lower normal stress tracks at later sliding and greater displacement (e.g., Figure 8, Barbery et al., 2021). These characteristics indicate significant plowing and production of wear products that contribute to changes in true area of contact with progressive slip.

We have investigated the hypothesis that the development of mm-scale hot spots evident in thermographs of machined samples (with and without grooves) reflect local differences in surface characteristics for both the moving surface that is imaged and the opposing stationary surface in contact. Main differences include the roughness features produced by machining and the distribution of the three main mineral phases of the granite (feldspar, quartz and biotite) that have different elastic and hardness properties (Fig. 3). In general, both mineral distribution and roughness features are relatively homogeneous and isotropic (Fig. 3a and 3c). At the grain scale, however, some clustering of like minerals occurs at the several-mm scale. Comparison of mineral maps and surface height indicate weak correlations between quartz and greater heights, and feldspar and lower heights (Fig. 3a, b). In addition, comparing pre-sliding mineral maps with thermographs document a correlation between high-temperature spots and mineral type; specifically, we find that feldspar and quartz show greater probability and biotite the lowest probability of coinciding with hot spots, and the relative probability qualitatively correlates with elastic moduli for the three minerals. Observations also indicate that after several sequential friction tests, wear produces gouge layers up to >50 μm thick with a corrugated interfacial slip surface, whereas the worn rock-surface bounding the gouge layer displays a more isotropic, homogeneous roughness.

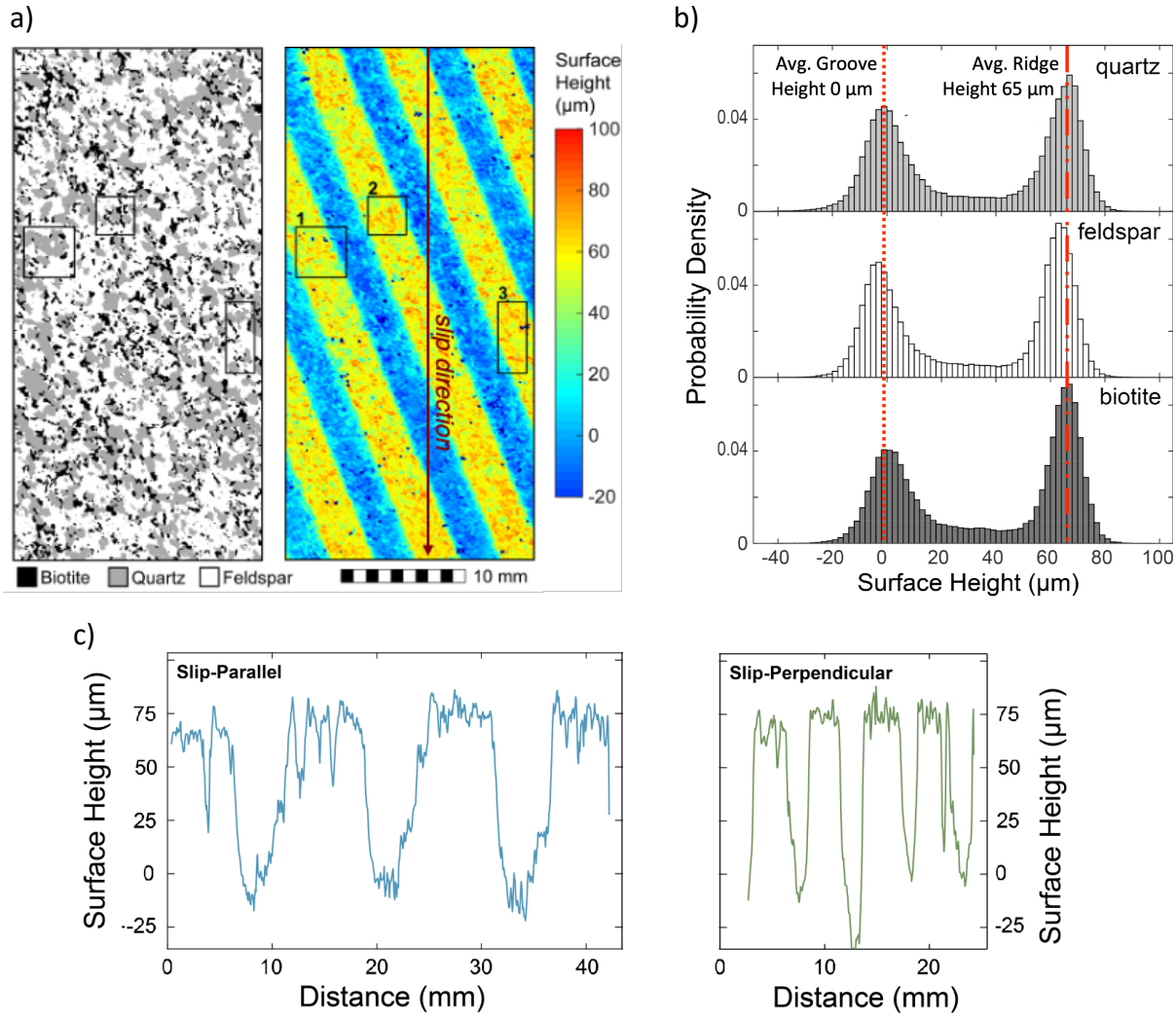

Figure 3. Mineral distribution and surface heights of the machined sliding surfaces of westerly granite are characterized prior to conducting high-speed sliding experiments to understand the influence of mineral grains and surface roughness on the size and location of hot spots developed during high-speed sliding. a) A Micro XRF spectrometer is used to determine elemental concentrations on the machined sliding surface to map the distribution of the dominant minerals (feldspar, quartz and biotite) exposed at the surface. A laser profilometer, with spot size of ~50 µm and resolution of 1 µm, is used to characterize the surface heights of the same machined surface. The machined ridges (yellow-red) and grooves (aqua-blue) are apparent. Numbered boxes highlight the visual correlation of mineral type and the local surface height. b) Surface height distributions indicate a greater probability of local highs on quartz grains than on feldspar grains. c) Surface-height profiles, both parallel and perpendicular to slip, show two dominant scales of roughness, a longer wavelength roughness associated with the machined grooves and ridges, and the smaller wavelength associated with the surfaces on the ridge tops and groove bottoms. The amplitude to wavelength ratios are similar for the two scales of roughness, and similar to that of observed for natural fault slip-surfaces.

References

Archard, J. F. (1959). The temperature of rubbing surfaces, Wear, 2, Issue 6,1959, Pages 438-455,ISSN 0043-1648,https://doi.org/10.1016/0043-1648(59)90159-0.

Barbery, M. R., F. M. Chester, and J. S. Chester (2021), Characterizing the distribution of temperature and normal stress on flash heated granite surfaces at seismic slip rates. *Journal of Geophysical Research: Solid Earth*, 126, e2020JB021353. https://doi.org/10.1029/2020JB021353.

Beeler, N. M., T. E. Tullis, and D. L. Goldsby (2008). Constitutive relationships and physical basis of fault strength due to flash heating. Journal of Geophysical Research 113(B1).

Dieterich, J. H. (1978). Time-dependent friction and mechanics of stick-slip. Pure Appl. Geophys. 116, 790-806.

Dieterich, J. H., and B. D. Kilgore (1994). Direct observation of frictional contacts: New insights for state-dependent properties. Pure and Applied Geophysics 143(1): 283-302.

Dieterich, J. H., and B. D. Kilgore (1996). Imaging surface contacts: power law contact distributions and contact stresses in quartz, calcite, glass and acrylic plastic. Tectonophysics 256: 219-239.

Logan, J.M., and L. W. Teufel (1986). The effect of normal stress on the real area of contact during frictional sliding in rocks. PAGEOPH, Vol. 124, No. 3: 471-485.

Rice, J. R. (2006). Heating and weakening of faults during earthquake slip. Journal of Geophysical Research 111(B5).

Rice, J.R., and Ruina, A.L. (1983). Stability of steady frictional slipping. J. Applied Mechanics. Vol. 50, 343-349.